



Contents lists available at ScienceDirect

International Journal of Biological Macromolecules

journal homepage: <http://www.elsevier.com/locate/ijbiomac>

Structural characterization and anti-inflammatory activity of alkali-soluble polysaccharides from purple sweet potato

Hong Chen^{a,1}, Jian Sun^{b,c,1}, Jun Liu^{a,*}, Yarun Gou^a, Xin Zhang^a, Xiaonan Wu^a, Rui Sun^a, Sixue Tang^a, Juan Kan^a, Chunlu Qian^a, Nianfeng Zhang^a, Changhai Jin^{a,*}^a College of Food Science and Engineering, Yangzhou University, Yangzhou 225127, Jiangsu, China^b College of Chemistry and Chemical Engineering, Yangzhou University, Yangzhou 225002, Jiangsu, China^c Xuzhou Institute of Agricultural Sciences in Jiangsu Xuhuai Area, Xuzhou 221131, Jiangsu, China

ARTICLE INFO

Article history:

Received 2 February 2019

Received in revised form 21 February 2019

Accepted 19 March 2019

Available online xxx

Keywords:

Alkali-soluble polysaccharide

Anti-inflammation activity

Structural characterization

Purple sweet potato

ABSTRACT

In this study, the structural characterization and anti-inflammation effect of dilute alkali-soluble polysaccharides from purple sweet potato were investigated. Three fractions (F-1, F-2 and F-3) were obtained by purifying crude polysaccharides on DEAE-52 cellulose column. The main fraction (F-1) was further purified on Sephadex G-200 column to afford purified alkali-soluble sweet potato polysaccharide (ASPP). The chemical structure of ASPP was analyzed by gas chromatography, Fourier transform infrared spectroscopy, methylation analysis and nuclear magnetic resonance spectroscopy. Monosaccharide compositional analysis showed ASPP was composed of rhamnose, arabinose, xylose, mannose and glucose in the molar ratio of 2.8:1.9:1.0:7.6:53.3. Moreover, the backbone of ASPP was composed of 1,4-linked Glcp with side chains attached to the O-6 position. The anti-inflammation effect of ASPP was further investigated by *in vitro* and *in vivo* experiments. Results showed ASPP could inhibit the levels of nitric oxide, interleukin (IL)-6, IL-1 β and TNF- α but increase the production of IL-10 in lipopolysaccharide (LPS)-treated RAW 264.7 macrophage cells. In addition ASPP could reduce the secretion of IL-6, IL-1 β and TNF- α in LPS-treated mice. Our results suggest ASPP can be developed as a novel anti-inflammation agent.

© 2019 Elsevier B.V. All rights reserved.

1. Introduction

Inflammation, including acute and chronic types, is the consequence of tissue injury, malfunction, stress and infections. Chronic inflammation can increase the probability of cancer, atherosclerosis and cardiovascular diseases. The mast cells and macrophages at inflamed tissues can engender inflammatory mediators such as interleukins (IL) and tumor necrosis factor- α (TNF- α) [1]. Currently, several *in vitro* and *in vivo* studies have demonstrated that natural polysaccharides possess anti-inflammatory effects [2–7].

In recent years, natural polysaccharides have gained increasing attentions for valuable pharmacological activities without causing significant side effects. It has been reported that polysaccharides isolated from different natural resources displayed antioxidant [8], antitumor [9], analgesic [10], anti-inflammatory [11], immunomodulatory [12] activities. In general, these functional properties of polysaccharides are closely related with their chemical structures [13].

Purple sweet potato is one member of sweet potato, which belongs to the family *Convolvulaceae* [14]. Yuan et al. [15] isolated a polysaccharide from sweet potato tuber and elucidated the polysaccharide was composed of rhamnose, glucose and galactose. Wu et al. [14] revealed that purple sweet potato polysaccharide is a promising natural antioxidant and antitumor agents. Yong et al. [16] found the purple sweet potato could be used to prepare antioxidant and intelligent pH-sensing films in active food packaging. In our previous studies, we isolated water-soluble, dilute alkali-soluble and concentrated alkali-soluble polysaccharides from purple sweet potato [17,18]. The crude polysaccharides from purple sweet potato were demonstrated to possess potential antioxidant activity, hepatoprotective effect against CCl₄-induced acute injury and immunomodulatory activity.

In this study, dilute alkali-soluble polysaccharides were isolated from purple sweet potato and purified on DEAE-52 cellulose and Sephadex G-200 columns. For the first time, the detailed chemical structure and anti-inflammatory activity of alkali-soluble sweet potato polysaccharide (ASPP) were investigated. The structure of ASPP was characterized by gas chromatography (GC), Fourier transform infrared (FT-IR) spectroscopy, methylation analysis and nuclear magnetic resonance (NMR) spectroscopy. The *in vitro* and *in vivo* anti-inflammatory activities of ASPP were further evaluated by lipopolysaccharide (LPS)-

* Corresponding authors.

E-mail addresses: junliu@yzu.edu.cn (J. Liu), chjin@yzu.edu.cn (C. Jin).¹ The co-first author.

induced RAW 264.7 cells and LPS-treated mice models, respectively. Our results are useful to establish the structure-function relationships of ASPP and facilitate the application of ASPP in food and pharmaceutical industries.

2. Materials and methods

2.1. Materials and chemicals

Purple sweet potato (variety of Xuzi No. 3) was purchased from Xuzhou Institute of Agricultural Sciences in Jiangsu Xuhuai Area (Xuzhou, China). Macroporous resin (AB-8) was obtained from Chemical Plant of Nankai University (Tianjin, China). DEAE-cellulose 52 and Sephadex G-200 resins were purchased from Whatman (Maidstone, UK) and Pharmacia (Uppsala, Sweden) Companies, respectively. Dulbecco's modified Eagle's medium (DMEM) and fetal bovine serum (FBS) were purchased from Gibco Invitrogen Co. (Carlsbad, CA). LPS from *Escherichia coli* O111: B4, 3-(4,5-dimethylthiazol-2-yl)-2,5-diphenyltetrazolium bromide (MTT) and dimethyl sulphoxide (DMSO) were purchased from Sigma-Aldrich Co. (St. Louis, MO). Enzyme-linked immunosorbent assay (ELISA) kits for IL-1 β , IL-6, TNF- α , IL-10 and Griess reagent for nitrite oxide (NO) were obtained from Nanjing Senbeijia Bioengineering Institute (Nanjing, China). All other chemicals and reagents were analytical and purchased from Sinopharm Chemical Reagent Co., Ltd. (Shanghai, China).

2.2. Isolation and purification of the alkali soluble polysaccharide (ASPP) from purple sweet potato

ASPP was extracted from purple sweet potato according to previously reported method [19]. Briefly, purple sweet potato powder was first defatted with 95% of ethanol (v/v), and was extracted with deionized water at 70 °C for 2 h and 0.5 mol/L sodium hydroxide solution at 60 °C for another 2 h. After cooling, the pH of mixture was adjusted to 7.0 using 0.5 mol/L hydrochloric acid solution and then centrifuged at 8000g for 15 min. The supernatant was deproteinated by Sevag method, followed by decolorization using AB-8 macroporous resin [20]. The extract solution was dialyzed (Mw cutoff = 3000 Da) against deionized water for 3 days and then freeze-dried to gain crude polysaccharides. The crude polysaccharides were re-dissolved in distilled water and purified on DEAE-52 cellulose column (4.6 cm \times 50 cm), which was sequentially eluted with distilled water, 0.1, 0.3 and 0.5 mol/L NaCl at 1 mL/min. The fractions were measured by phenol-sulphuric acid method [21]. The major polysaccharides fractions (namely F-1, F-2 and F-3) were collected, dialyzed, concentrated and lyophilized for further analysis. The main fraction of F-1 was further purified on Sephadex G-200 column (3 cm \times 100 cm) with distilled water at a flow rate of 0.2 mL/min to obtain purified polysaccharide fraction, which was named as ASPP.

2.3. Structural characterization of ASPP

2.3.1. Monosaccharide composition analysis

The monosaccharide composition of ASPP was performed according to the method of Zhu et al. [22]. ASPP (5 mg) was dissolved in 4 mL of 2 M trifluoroacetic acid (TFA) and heated at 95 °C for 10 h. The excess TFA was removed by evaporation with methanol under vacuum. The hydrolyzate was reduced by NaBH₄ at 60 °C for 1 h and evaporated to dryness, followed by incubation with acetic anhydride and pyridine (v/v = 1:1) at 100 °C for 1 h. The obtained alditol acetates were analyzed on GC (Agilent Technologies, CA, USA) equipped with flame ionization detector (FID) and HP-5 capillary column (30 m \times 0.32 mm, 0.25 μ m). The column temperature was programmed from 70 °C to 210 °C at 10 °C/min (held for 1 min), and increased to 235 °C at 5 °C/min (held for 2 min), and then increased to 250 °C at 10 °C/min (held for 1 min), and finally increased to 280 °C at 15 °C/min for 1 min. Nitrogen gas was used

as the carrier gas and was set at 0.7 mL/min. The temperatures of injector and detector were 250 and 300 °C, respectively.

2.3.2. Molecular weight analysis

The molecular weight of ASPP was determined by high performance gel permeation chromatography (HPGPC) on Agilent 1200 system (Agilent Technologies, CA, USA) equipped with TSK-gel G4000 PW_{XL} column (300 mm \times 7.8 mm) and evaporative light scattering detector (ELSD) [20]. The column and detector were maintained at 40 °C. Sample solution (20 μ L, 2 mg/mL) was injected into the system and eluted with 50 mmol/L NaCl at a flow rate of 0.5 mL/min. Molecular weight of ASPP was estimated through the standard curve established by T-series dextran standards (T-500, T-200, T-100, T-50 and T-10).

2.3.3. Fourier-transform infrared (FT-IR) spectroscopy analysis

ASPP was mixed with dried KBr powder, pressed into 1 mm thick disk and analyzed on Varian 670 FT-IR spectrophotometer (Varian Inc., CA, USA). The FT-IR spectrum was recorded in the range of 4000–400 cm⁻¹.

2.3.4. Methylation and GC-MS analysis

Methylation analysis of ASPP was performed according to the previously reported method [20]. Dried ASPP (70 mg) was dissolved completely in DMSO (10 mL) with addition of NaOH powder (100 mg), which was reacted at 20 °C for 1 h. Then CH₃I (2 mL) was added slowly into the solution and further reacted for 1 h. Finally, 2 mL of distilled water was added to terminate the reaction. The solution was dialyzed (Mw cut off = 3600 Da) in deionized water for 3 days and then freeze-dried to gain methylated polysaccharide. The methylation reaction was repeated for four times until the polysaccharide was completely methylated, which was confirmed by the disappearance of O—H band at 3200–3700 cm⁻¹ in FT-IR spectrum.

The methylated polysaccharide was dissolved in 4 mL of 2 M trifluoroacetic acid (TFA) and heated at 95 °C for 10 h. The hydrolyzate was dissolved in 2 mL distilled water, reduced by NaBH₄ at 60 °C for 1 h and evaporated to dryness. Then, 1.5 mL of acetic anhydride and 1.5 mL of pyridine were added into the system and reacted at 100 °C for 1 h. The reaction products were subjected to GC-MS analysis (Thermo Fisher Scientific, Waltham, MA, USA) equipped with HP-5 MS column (30 m \times 250 μ m, 0.25 μ m). The initial column temperature was 50 °C (held for 5 min) and then increased to 250 °C at 15 °C/min (held for 5 min). The partially methylated alditol acetates were identified by their relative retention times and MS fragmentation patterns.

2.3.5. NMR analysis

ASPP (50 mg) was dissolved in 0.5 mL of D₂O. The 1D and 2D NMR spectra including ¹H NMR, ¹³C NMR, ¹H/¹H homonuclear correlation spectroscopy (COSY), nuclear overhauser enhancement spectroscopy (NOESY), heteronuclear single quantum coherence (HSQC) and heteronuclear multiple-bond coherence (HMBC) were recorded by AVANCE-600 NMR spectrometer (Bruker Inc., Rheinstetten, Germany) at 25 °C.

2.4. Measurement of the cytotoxicity of ASPP

RAW264.7 cells were obtained from the cell bank of Chinese Academy of Science (Shanghai, China) and were grown in DMEM media supplemented with 10% of heat-inactivated fetal bovine serum (FBS), 100 U/mL of penicillin and 100 μ g/mL of streptomycin at 37 °C under a humidified incubator containing 5% of CO₂. Effect of ASPP on the viability of RAW264.7 macrophage cells were measured via MTT assay. Briefly, cells were cultivated in a 96-wells plate at a concentration of 1 \times 10⁵ cells/mL overnight. Different concentrations of ASPP were added into 96-wells plate and cultured for 24 h. Then, the culture supernatant was discarded and 10 μ L of MTT (5 mg/mL) was added. After reaction for 4 h, the colored formazan was dissolved by addition of 100 μ L of DMSO. The absorbance of reaction solution at 570 nm was measured by a

microplate reader (Varioskan Flash, Thermo Scientific, USA). The cell viability was calculated according to the formula:

$$\text{Cell viability (\%)} = (A_s/A_c) \times 100 \quad (1)$$

where A_s and A_c represented the absorbance of sample group and normal control group, respectively.

2.5. Measurement of the *in vitro* anti-inflammatory activity of ASPP

2.5.1. Experimental models

The anti-inflammation effect of ASPP was assessed by two different experimental models [23]. Model A: to evaluate anti-inflammatory potential of ASPP on RAW264.7 macrophages stimulated by LPS. RAW264.7 macrophages were cultured with LPS (1 $\mu\text{g}/\text{mL}$) and different concentrations of ASPP samples (250, 500, 1000 and 2000 $\mu\text{g}/\text{mL}$) for 48 h. Model B: to examine the curative effect of ASPP on the inflammation induced by LPS. RAW264.7 macrophages were firstly cultured with LPS (1 $\mu\text{g}/\text{mL}$) in 96-wells plate for 24 h, and then LPS was removed by discarding the supernatant. Finally, different concentrations of ASPP samples (250, 500, 1000 and 2000 $\mu\text{g}/\text{mL}$) were added into 96-wells plate for another 24 h.

2.5.2. Measurement of nitric oxide (NO) release

The concentration of NO in supernatant was determined by Griess reagent. Briefly, 50 μL of cell culture medium was mixed with 50 μL of Griess reagent I (5% phosphoric acid containing 1% sulphanilamide) and 50 μL of Griess reagent II (0.1% *N*-1-naphthyl-enediamide dihydrochloride in distilled water) and placed at room temperature for 30 min. The absorbance of reaction mixture was read at 540 nm using a microplate reader. NO concentration was calculated according to the standard curve of sodium nitrite.

2.5.3. Measurement of pro-inflammatory and anti-inflammatory cytokines production

After incubation, cell supernatant was collected to determine the levels of pro-inflammatory (IL-1 β , IL-6, TNF- α) and anti-inflammatory (IL-10) cytokines by using ELISA kits according to manufactures' instructions. The absorbance of reaction mixture was read at 540 nm by a microplate reader.

2.6. Measurement of the *in vivo* anti-inflammatory activity of ASPP

2.6.1. Animals and treatments

A total of 48 female ICR mice (18–20 g, 4 weeks old) were obtained from the Comparative Medical Center of Yangzhou University (Yangzhou, China), maintained at $20 \pm 2^\circ\text{C}$ with 12 h light-dark cycles and were free to access standard chow (Xietong Co., Nanjing, China) and water for one week. All experiments were conducted according to the Guidelines for the Care and Use of Laboratory Animals issued by the People's Republic of China, and were approved by the Ethics Committee of Experimental Animal Care at Yangzhou University (permit No. SYXK2016-0019). Mice were randomly divided into four groups ($n = 12$) including normal, LPS, normal + ASPP and LPS + ASPP treatment groups. The LPS and LPS + ASPP groups were intraperitoneally injected with LPS (0.5 mg/kg) on days 5, 6 and 7 [24]. The normal + ASPP and LPS + ASPP groups were given ASPP (400 mg per kg BW) and the other two groups were given saline by gavage once daily. On the 30th day, the mice were weighed and sacrificed by cervical dislocation.

2.6.2. Measurement of the levels of cytokines (IL-1 β , IL-6, TNF- α and IL-10) in liver and serum

The levels of IL-1 β , IL-6, TNF- α and IL-10 in the liver and serum of mice were analyzed by ELISA Kits according to the manufacturer's instructions.

2.7. Statistical analysis

All the data were expressed as mean \pm standard deviation (SD). Statistical analysis was performed via SPSS software (version 17.0, Chicago, IL, USA).

3. Results and discussions

3.1. Isolation, purification and molecular weight of ASPP

The extraction yield of crude dilute alkali-soluble polysaccharide from purple sweet potato was 4.29%. After decolorization and deproteinization, the crude polysaccharide was loaded onto DEAE-52 cellulose column and three fractions including F-1, F-2 and F-3 were

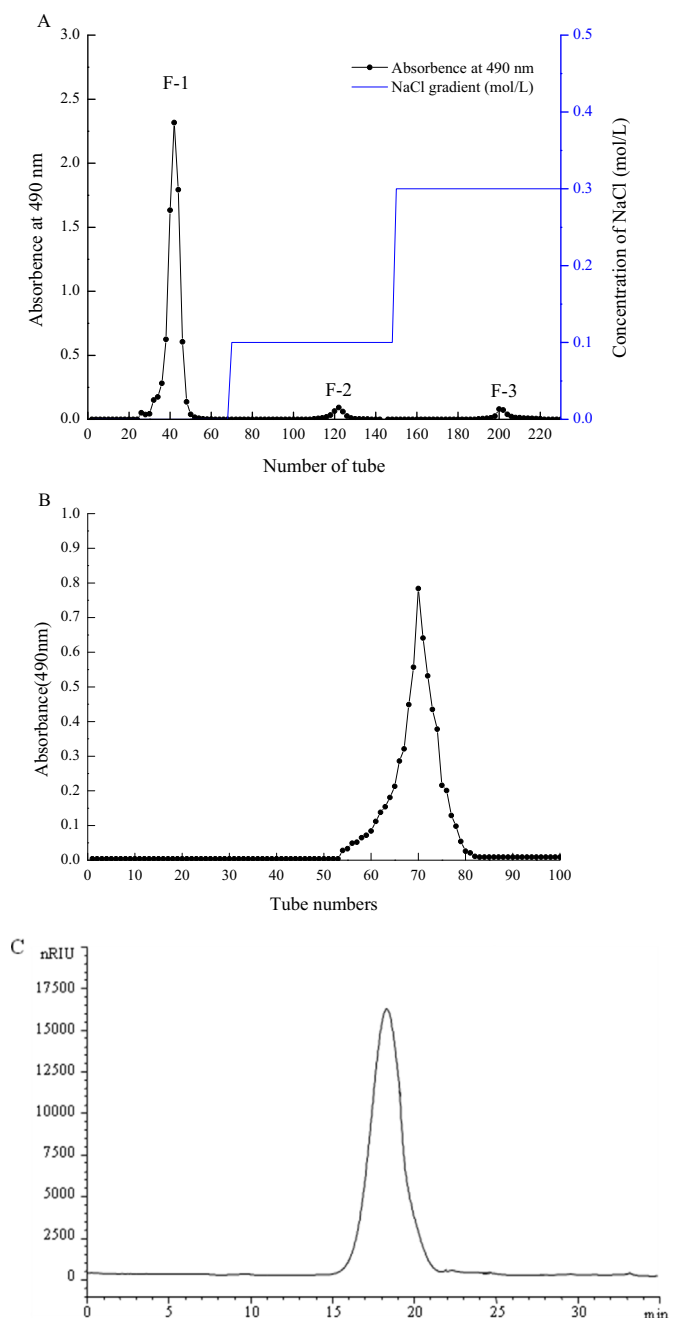


Fig. 1. Anion-exchange chromatogram of crude polysaccharides on DEAE-52 column (A) and the main fraction of F-1 on Sephadex G-200 column (B) and HPGPC profile of ASPP (C).

obtained (Fig. 1A). The main fraction of F-1 was further subjected to Sephadex G-200 gel filtration column to afford ASPP (Fig. 1B). The purity and molecular weight of ASPP was measured by HPGPC system. There is only one single peak on the column, suggesting ASPP was a homogeneous polysaccharide (Fig. 1C). The molecular weight of ASPP was determined as 1.8×10^5 Da based on the standard curve of dextran T-series. Wu et al. [14] found that three water-soluble polysaccharide fractions from purple sweet potato showed molecular weights of 3.33×10^4 , 1.78×10^4 and 7.53×10^4 Da, respectively. The difference in the molecular weights of alkali-soluble and water-soluble polysaccharides might be due to different extraction methods used.

3.2. Structural characterization of ASPP

3.2.1. Monosaccharides composition of ASPP

Monosaccharide composition analysis showed ASPP was composed of rhamnose, arabinose, xylose, mannose and glucose in the molar ratio of 2.8: 1.9: 1.0: 7.6: 53.3 (Fig. 2A and B). Sun et al. [18] also found that crude alkali-soluble polysaccharide extracted from purple sweet potato was mainly composed of glucose.

3.2.2. FT-IR spectrum

The FT-IR spectrum of ASPP is shown in Fig. 3. The distinctive broad band at 3429 cm^{-1} was due to the vibration of O—H [25]. The weak band at 2931 cm^{-1} was attributed to the stretching vibration of C—H [26]. The strong absorption bands around 1413 and 1387 cm^{-1} indicated the vibrations of C—H [26]. Besides, three bands at 1147 , 1078 and 1024 cm^{-1} indicated the presence of pyranoside, and the peak at 858 cm^{-1} indicated that the presence of α -type glycoside [27]. In addition, the weak band at 914 cm^{-1} suggested that the presence of the β -type glycoside [25]. The weak band at 613 cm^{-1} was assigned to C—C stretching [28]. Sun et al. [18] and Wu et al. [14] also found that β -type glycoside in the polysaccharides isolated from purple sweet potato.

3.2.3. Methylation analysis

To determine the linkage patterns of monosaccharides, ASPP was methylated and analyzed by GC-MS. As shown in Table 1, eight partially

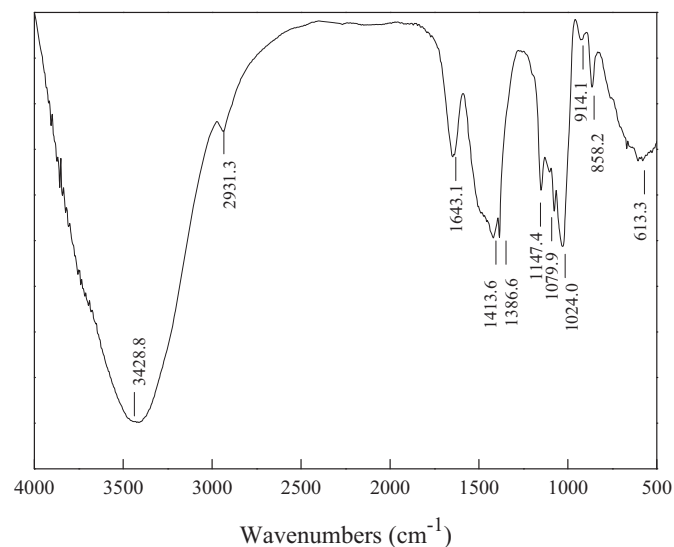


Fig. 3. FT-IR spectra of ASPP.

methylated alditol acetates were identified, namely 2,3,6-tri-Me-glucitol, 2,3-di-Me-glucitol, 2,3,4,6-tetra-Me-rhamnitol, 2,3-di-Me-rhamnitol, 2,3,4,6-tetra-Me-mannitol, 2,3,5-tri-Me-arabitol, 2,3,4-tri-Me-xylitol and 2,3,4,6-tetra-Me-glucitol. Obviously, the major derivative was 2,3,6-tri-Me-glucitol (42.44%), indicating ASPP was mainly composed of 1,4-linked glucopyranosyl residues.

3.2.4. NMR

The structure of ASPP was further investigated by 1D and 2D NMR analysis. According to the ^1H NMR of ASPP (Fig. 4A), the chemical shift at 5.32 ppm (H-1) should be α -linked residue (residue A). According to the cross-peaks of COSY spectrum (Fig. 4C), the H-2, H-3, H-4, H-5, H-6 and H-6' of residue A were successively identified at 3.56 , 3.88 , 3.58 , 3.77 , 3.84 and 3.68 ppm , respectively. Then the signals at 99.64 ,

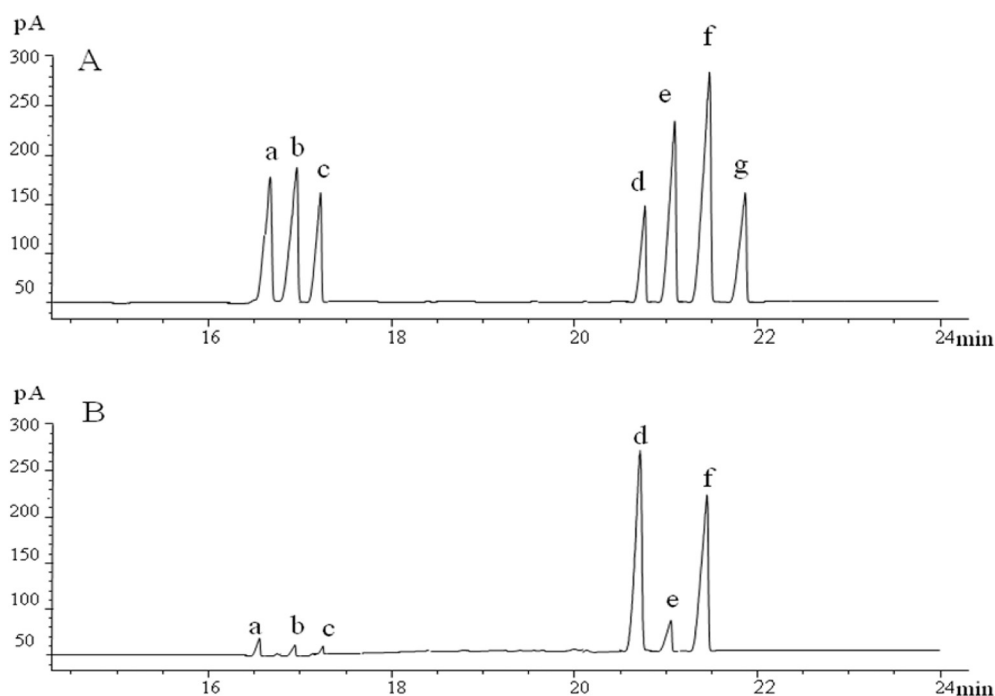


Fig. 2. GC chromatograms of standard monosaccharides (A) and monosaccharide composition of ASPP (B) (peaks: a, rhamnose; b, arabinose; c, xylose; d, inositol; e, mannose; f, glucose; g, galactose).

Table 1
Methylation analysis of ASPP.

Retention time (min)	Linkage pattern	Partial methylated alditol acetates	Mass fragments (<i>m/z</i>)	Molar percentages (%)
11.54	→4)-Rhap-(1→	2,3-Me ₂ -Rhap	43, 45, 57, 60, 81, 91, 105, 135, 145, 163, 191, 205	0.43
13.13	GlcP-(1→	2,3,4,6-Me ₄ -GlcP	43, 45, 57, 71, 87, 101, 117, 129, 161, 191, 206	10.71
13.94	Rhap-(1→	2,3,4,6-Me ₃ -Rhap	43, 71, 89, 101, 117, 131, 133, 161, 175	5.08
14.65	Xylp-(1→	2,3,4-Me ₃ -Xylp	43, 57, 71, 85, 97, 117, 135, 162	0.21
17.00	Manp-(1→	2,3,4,6-Me ₄ -Manp	43, 45, 71, 87, 101, 113, 117, 129, 145, 161, 205	8.06
17.09	→4)-6-GlcP-(1→	2,3-Me ₂ -GlcP	43, 57, 71, 85, 99, 117, 127, 155, 207, 261	29.13
18.51	→4)-GlcP-(1→	2,3,6-Me ₃ -GlcP	43, 57, 71, 87, 99, 113, 117, 129, 145, 161, 205	42.44
18.86	Araf-(1→	2,3,5-Me ₃ -Araf	43, 57, 71, 87, 99, 101, 117, 129, 161	3.94

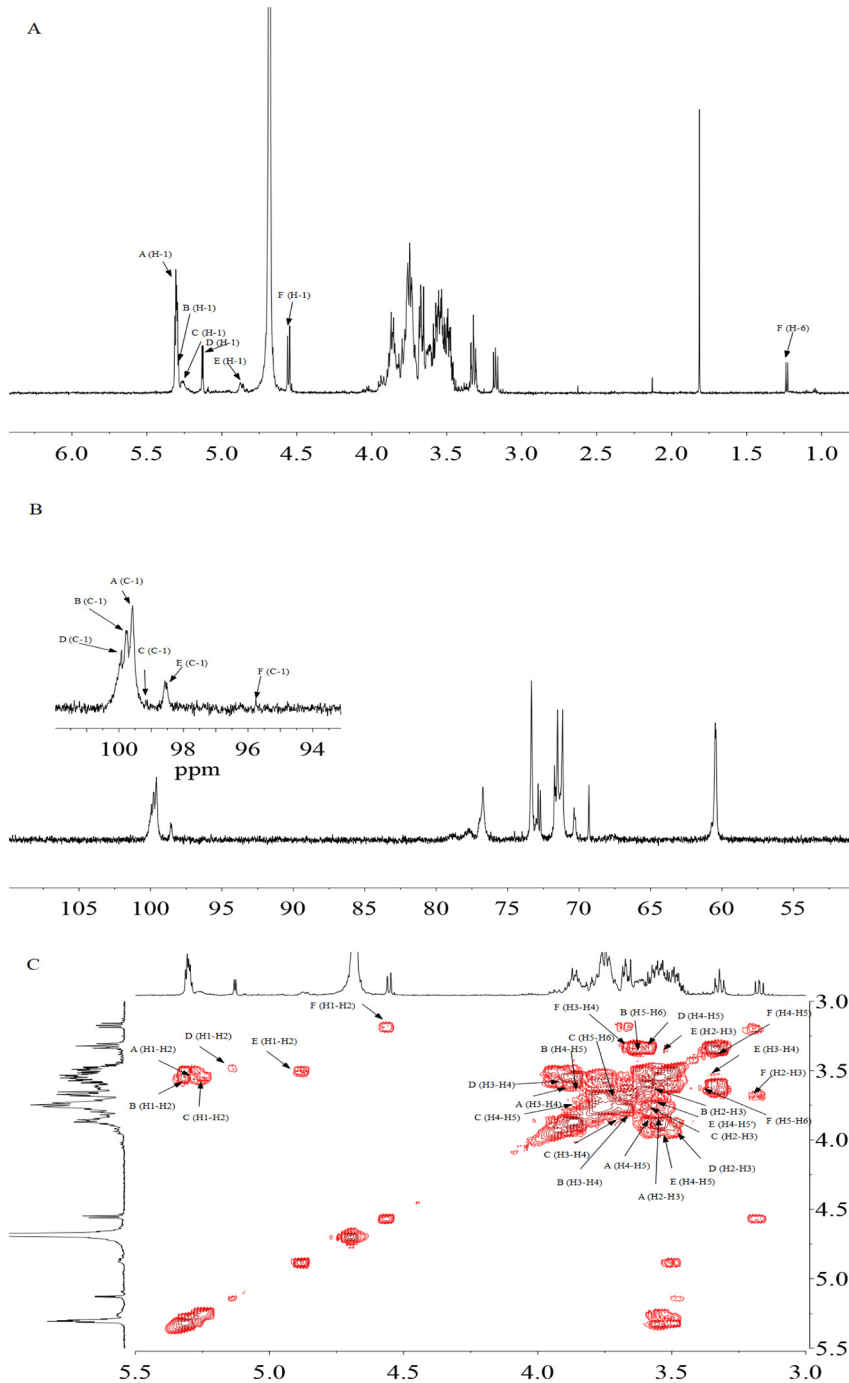


Fig. 4. ¹H NMR (A), ¹³C NMR (B); COSY (C); HSQC (D); HMBC (E) and NOESY (F) spectra of ASPP.

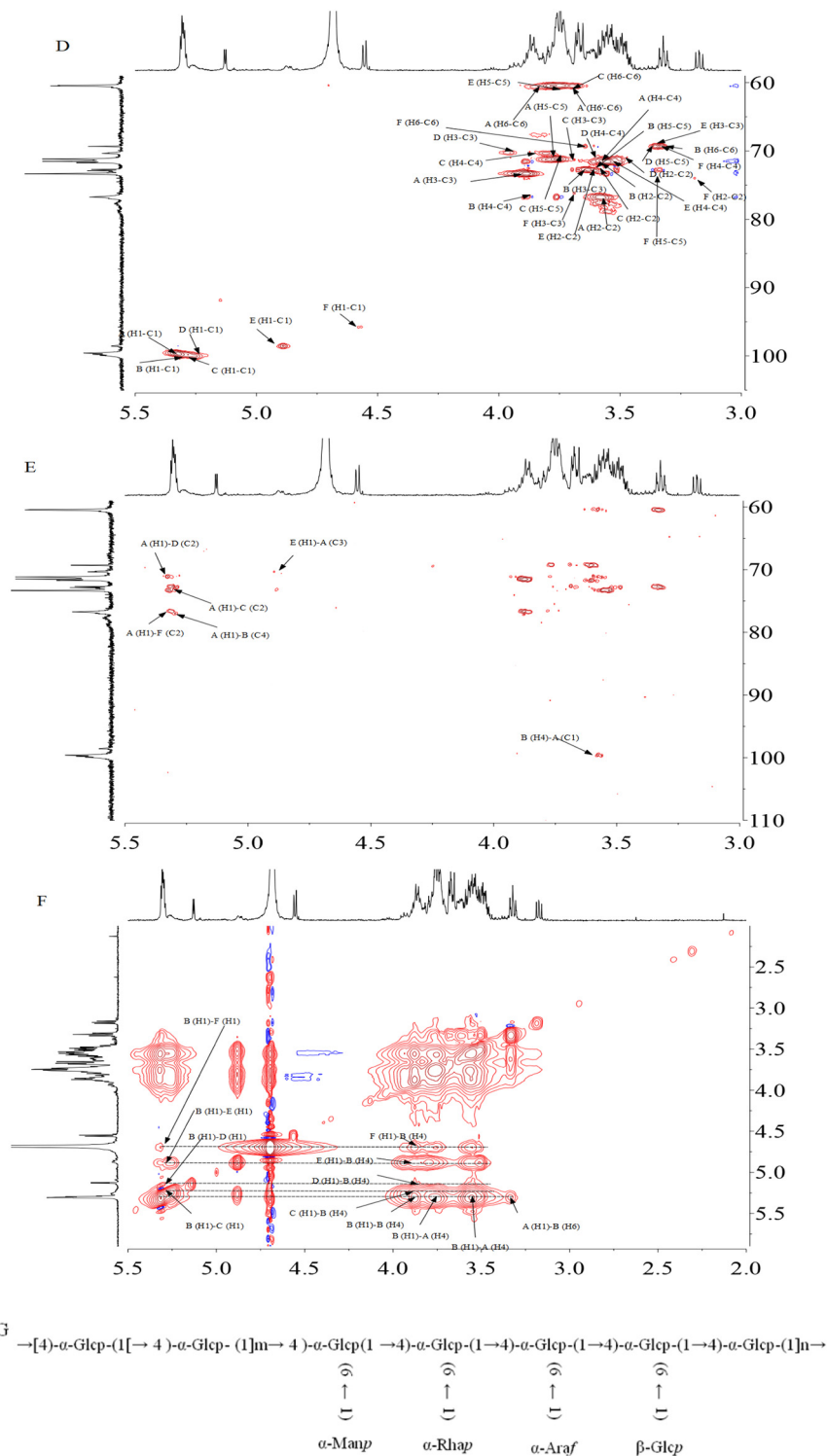


Fig. 4 (continued).

71.49, 73.17, 76.79, 71.23 and 60.51 ppm were determined as C-1, C-2, C-3, C-4, C-5 and C-6 of residue A, owing to ^{13}C NMR and HSQC spectra (Fig. 4B and D). According to methylation analysis and literature [29], residue A was identified as $\rightarrow 4)\text{-}\alpha\text{-D-Glcp-(1}\rightarrow$. For residue B, its H-1 signal was at 5.28 ppm. From COSY spectrum (Fig. 4C), the H-2 of residue B was determined at 3.58 ppm because of its correlation with H-1 (5.28 ppm). Likewise, the H-3, H-4, H-5 and H-6 were successively determined at 3.66, 3.85, 3.62 and 3.34 ppm, respectively. According to

HSQC spectrum (Fig. 4D), the C-1, C-2, C-3, C-4, C-5 and C-6 of residue B were determined at 99.77, 71.49, 72.47, 76.79, 72.91 and 69.42 ppm, respectively. Based on the results of methylation and literature [29], residue B was determined as $\rightarrow 4)\text{-}6\text{-}\alpha\text{-D-Glcp-(1}\rightarrow$. Other residues' signals were assigned in the same way. All proton and carbon signals of each residue are summarized in Table 2. However, the signals of some residues detected by GC-MS (such as Xylp-(1 \rightarrow and $\rightarrow 4)\text{-Rhap-(1}\rightarrow$) were not detected by NMR spectroscopy, possibly due to their low

Table 2
Summary of ^1H and ^{13}C chemical shifts for ASPP.

Residues	Chemical shift assignments of ASPP							
		1	2	3	4	5	6	
A	$\rightarrow 4$)- α -D-Glcp-(1 \rightarrow	H	5.32	3.56	3.88	3.58	3.77	3.84/3.68
		C	99.64	71.49	73.17	76.79	71.23	60.51
B	$\rightarrow 4$)-6- α -D-Glcp-(1 \rightarrow	H	5.28	3.58	3.66	3.85	3.62	3.34
		C	99.77	71.49	72.47	76.79	72.91	69.42
C	α -D-Manp-(1 \rightarrow	H	5.23	3.59	3.69	3.87	3.74	3.72
		C	99.64	72.88	70.66	70.34	70.52	60.33
D	α -D-Rhap-(1 \rightarrow	H	5.14	3.48	3.93	3.59	3.33	1.24
		C	100.49	70.66	70.34	71.11	69.47	16.62
E	α -L-Araf-(1 \rightarrow	H	4.88	3.54	3.36	3.53	3.96/3.72	
		C	98.62	72.2	69.58	71.48	60.99	
F	β -D-Glcp-(1 \rightarrow	H	4.57	3.19	3.69	3.31	3.37	3.65/3.62
		C	95.89	74.02	76.39	69.12	73.17	69.21

molecular ratio in ASPP. The correlations of both inter- and intra-residues can be confirmed by the HMBC (Fig. 4E) and NOESY spectra (Fig. 4F). In the HMBC spectrum, a cross peak was observed between H-1 (5.32 ppm) and C-4 (76.79 ppm) of residue A, H-4 (5.58 ppm) of and C-1 (99.64 ppm) of residue A, which implied that the backbone structure of ASPP was mainly composed of $\rightarrow 4$)- α -D-Glcp-(1 \rightarrow (residue A). In the NOESY spectrum, the inter-residual cross-peaks of H-4 of residue B (3.85 ppm) and H-1 of residue C (5.23 ppm) indicated that α -D-Manp-(1 \rightarrow (residue C) was attached to the O-6 position of $\rightarrow 4$)-6- α -D-Glcp-(1 \rightarrow (residue B). Similarly, other residues including α -D-Rhap-(1 \rightarrow (residue D), α -L-Araf-(1 \rightarrow (residue E) and β -D-Glcp-(1 \rightarrow (residue F) were also identified to be linked to O-6 position of $\rightarrow 4$)-6- α -Glc-

(1 \rightarrow (residue B). Based on the described above analysis, ASPP was proved to be linear α -(1 $\rightarrow 4$)-glucan with terminal α -Manp, α -Rhap, β -Araf and β -Glc residues linked to the backbone at O-6 positions (Fig. 4G).

3.3. The cytotoxicity of ASPP

The cytotoxicity of ASPP on RAW264.7 macrophages was measured by MTT assay. As shown in Fig. 5A, ASPP have no acute cytotoxicity on RAW264.7 macrophage cells. Compared to the normal control group, 1000 $\mu\text{g}/\text{mL}$ of ASPP treatment could notably increase cell viability.

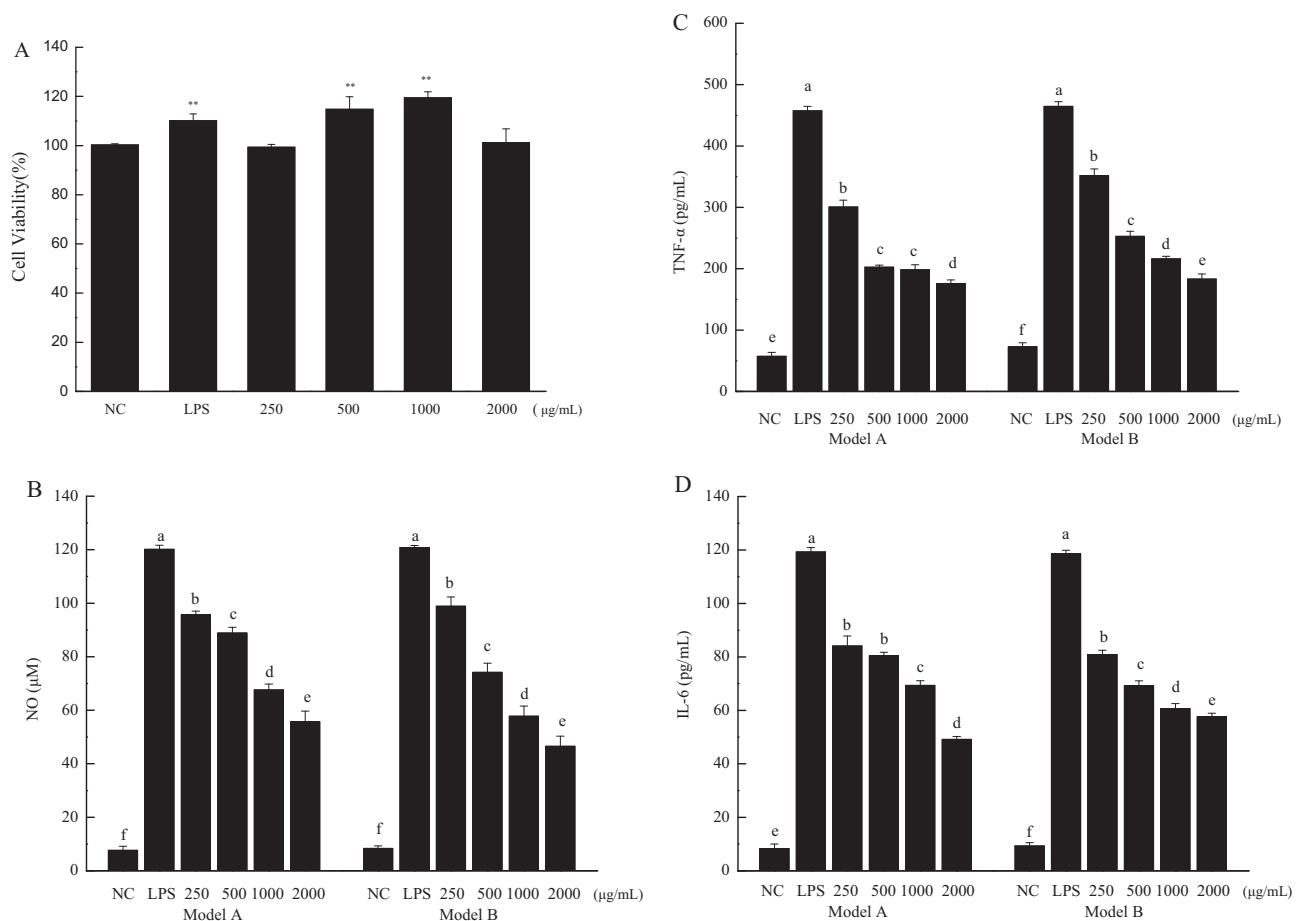


Fig. 5. Effect of ASPP on the viability of RAW264.7 cells (A) and the production of NO (B), TNF- α (C), IL-6 (D), IL-1 β (E) and IL-10 (F) by using Models A and B. Values are expressed as mean \pm SD ($n = 6$). Data marked with different letters (a-f) differ significantly ($p < 0.05$).

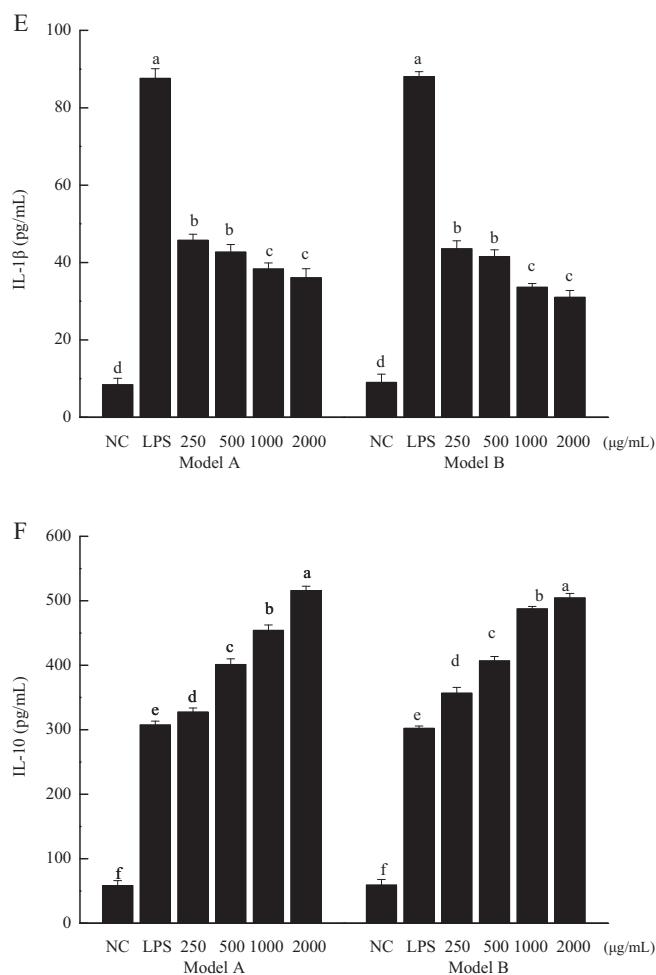


Fig. 5 (continued).

3.4. Anti-inflammatory activity of ASPP in LPS-stimulated RAW 264.7 cells

Macrophages play an important role in inflammation and immune responses. During inflammation, macrophages induce the expression of pro-inflammatory genes such as inducible nitric oxide synthase (iNOS). Accordingly, NO is produced from L-arginine by iNOS [30]. Therefore, NO production level is considered as one of the indicators of macrophage activation. LPS can stimulate macrophages and initiate inflammatory responses with production of inflammatory cytokines, such as IL-1 β , IL-6, TNF- α and IL-10 [31].

Model A was used to evaluate the anti-inflammatory potential of ASPP on RAW264.7 macrophages. NO production level was significantly enhanced by LPS ($p < 0.05$); however, ASPP treatment had a significant dose-dependent suppression effect on NO production (Fig. 5B). To further evaluate the anti-inflammatory effects of ASPP on LPS treated RAW264.7 cells, inflammatory cytokines including IL-1 β , IL-6, TNF- α

and IL-10 were determined by ELISA kits. As shown in Fig. 5C, D and E, IL-1 β , IL-6 and TNF- α production significantly increased in LPS treatment group ($p < 0.05$). However, these cytokines' production significantly decreased by ASPP treatment ($p < 0.05$). Meanwhile, there was no significantly difference in IL-1 β and IL-6 secretion between 250 and 500 $\mu\text{g/mL}$ of ASPP treatments ($p > 0.05$). There was also no notably difference in TNF- α secretion between 500 and 1000 $\mu\text{g/mL}$ of ASPP treatments ($p > 0.05$). ASPP notably enhanced the level of IL-10 as compared with normal control group ($p < 0.05$) (Fig. 5F). Above results suggested that ASPP had a mild anti-inflammatory potential on RAW264.7 macrophages. Sanjeeva et al. [32] reported that polysaccharide from *Sargassum horneri* inhibited the LPS-induced NO as well as pro-inflammatory cytokine (TNF- α and IL-6) production in RAW 264.7 cells through down-regulating nuclear factor- κB signaling cascade. Zhang et al. [33] found exopolysaccharides from *Auricularia auricula-judae* significantly increased IL-10 secretion.

Model B was used to examine the curative effect of ASPP on LPS-induced inflammation. Effect of ASPP on NO releasing level was shown in Fig. 5B. A significant decrease of NO production was observed in ASPP treatment group when compared with LPS treatment group ($p < 0.05$). Effects of ASPP on pro-inflammatory cytokine (IL-1 β , IL-6, TNF- α) and anti-inflammatory cytokine (IL-10) secretion by LPS-treated RAW264.7 macrophages were shown in Fig. 5C, D and F. As compared to LPS treatment group, ASPP treatment could dose-dependently suppress TNF- α , IL-1 β and IL-6 secretion; however, enhance IL-10 production in LPS-stimulated RAW264.7 macrophages ($p < 0.05$). These results suggested ASPP had a strong curative effect on LPS-induced inflammation. Lacerda et al. [34] found that polysaccharides from *Cabernet Franc*, *Cabernet Sauvignon* and *Sauvignon Blanc* wines could inhibit the production of NO, TNF- α and IL-1 β in LPS-stimulated RAW 264.7 cells. Wen et al. [23] found polysaccharides from *Sargassum horneri* have curative effect on inflammation. Our previous study found three crude polysaccharides (water soluble, dilute alkali soluble and concentrated alkali soluble polysaccharides) extracted from purple sweet potato had immunomodulatory functions [17]. Our present study further suggested that ASPP has anti-inflammatory activity on LPS-stimulated RAW264.7 macrophages via inhibiting pro-inflammatory cytokine production (IL-1 β , IL-6, TNF- α) and enhancing anti-inflammatory cytokine (IL-10) level.

3.5. Anti-inflammatory activity of ASPP in LPS-treated mice

3.5.1. Effect of ASPP on thymus and spleen indices

As shown in Table 3, mice in all groups showed similar initial body weights. However, mice in LPS and LPS + ASPP treatment groups showed significantly higher weight losses than other groups ($p < 0.001$). Moreover, the weight losses of mice in LPS treatment group were much higher than those of LPS + ASPP treatment group. Thymus and spleen are major immune organs and their mass indices can reflect the degrees of inflammation [24]. The spleen and thymus indices of mice treated with LPS displayed a remarkable difference compared to these of normal control group ($p < 0.001$), indicating that the celiac inflammation model was established successfully. Besides, the spleen indices were reduced by ASPP but did not reach the normal level.

3.5.2. Effect of ASPP on cytokines production

To study the protective effect of ASPP on LPS-treated mice, the levels of cytokines in liver and serum of all groups were determined. As shown in Fig. 6, levels of TNF- α , IL-1 β , IL-6 and IL-10 in the serum of normal and normal + ASPP treatment groups were almost the same ($p > 0.05$). As compared to the normal group, the levels of TNF- α , IL-1 β and IL-6 significantly increased but the level of IL-10 decreased in LPS treatment group ($p < 0.05$). The production of IL-1 β was significantly decreased in LPS + ASPP treatment group as compared to LPS treatment group ($p < 0.01$), indicating effective anti-inflammatory activity of ASPP. The production of cytokines such as TNF- α , IL-1 β , IL-6 and IL-10 in the

Table 3

Effects of ASPP on the body weight, thymus index and spleen index of normal, normal + ASPP, LPS and LPS + ASPP treated mice.

Group	Initial body weight (g)	Final body weight (g)	Thymus index (mg/g)	Spleen index (mg/g)
Normal	26.72 \pm 0.83	29.70 \pm 0.75	2.58 \pm 0.43	2.00 \pm 0.24
LPS	26.39 \pm 1.01	22.50 \pm 0.79***	1.22 \pm 0.25***	4.11 \pm 0.50***
Normal + ASPP	26.22 \pm 0.69	29.57 \pm 0.79	2.54 \pm 0.28	1.91 \pm 0.32
LPS + ASPP	26.38 \pm 1.60	25.87 \pm 1.06***	1.42 \pm 0.31***	2.99 \pm 0.39***

*** $p < 0.001$.

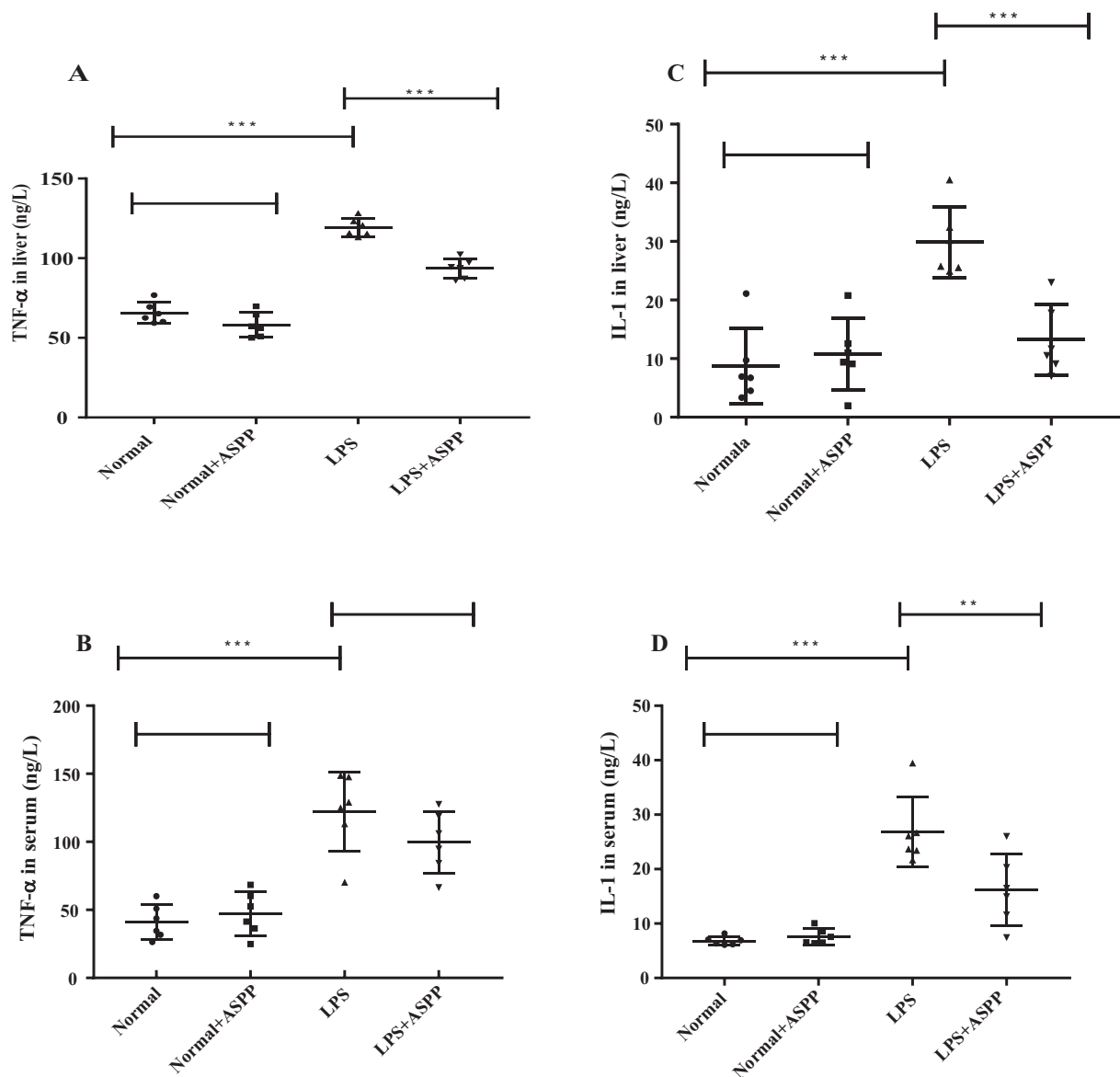


Fig. 6. Effect of ASPP on TNF- α levels in the liver (A) and serum (B); IL-1 β levels in the liver (C) and serum (D); IL-6 levels in the liver (E) and serum (F); IL-10 levels in the liver (G) and serum (H). Values are expressed as mean \pm SD.*: $p < 0.05$; **: $p < 0.01$; ***: $p < 0.001$.

liver was also assessed. The levels of TNF- α , IL-1 β and IL-6 in the liver homogenate were higher in LPS treatment group than those in the normal control group. LPS + ASPP treatment significantly suppressed the increase in the levels of TNF- α and IL-1 β in the liver as compared to LPS treatment ($p < 0.05$). However, the level of IL-10 was not significantly affected by LPS + ASPP treatment. Results suggested that ASPP have a mild anti-inflammatory activity on LPS-stimulated mice via inhibiting pro-inflammatory IL-1 β , IL-6 and TNF- α . Rajagopal et al. [35] reported that the polysaccharide from *Curcuma longa* could significantly inhibit pro-inflammatory mediators such as TNF- α and IL-8 and enhance anti-inflammatory mediators such as IL-10. Both nuclear factor- κ B (NF- κ B) and mitogen-activated protein kinases (MAPKs) signaling pathways are critical regulators of immune responses [36]. NF- κ B is considered as the major transcription factor, which regulates COX-2 and iNOS expression, NO and prostaglandin E2 (PGE2) production, and the release of pro-inflammatory cytokines (TNF- α , IL-1 β and IL-6). MAPKs pathway transfers information to the cell in the extracellular environment and ultimately to the nucleus [37]. Sanjeeva et al. [32] reported that the crude polysaccharide from *Sargassum horneri* (brown seaweed) exhibited anti-inflammatory effects via suppressing NF- κ B

and down regulating phosphorylation of ERK and p38 kinases in MAPKs signaling pathway. To elucidate the anti-inflammatory mechanisms of ASPP, further studies at the molecular levels are necessary.

4. Conclusions

A dilute alkali-soluble polysaccharide (ASPP) was extracted from purple sweet potato and purified by DEAE-52 cellulose and Sephadex G-200 column. The structure of ASPP was mainly composed of 1,4-linked Glcp as the backbone with side chains attached to the O-6 positions. The polysaccharide was found to have anti-inflammation effects by both *in vitro* and *in vivo* assays. Our results suggest ASPP can be applied as an effective anti-inflammatory agent. Further studies on the anti-inflammatory mechanisms of ASPP at the molecular levels are necessary.

Acknowledgements

This work was supported by National Natural Science Foundation of China (Nos. 31871803 and 31571788), Natural Science Foundation of

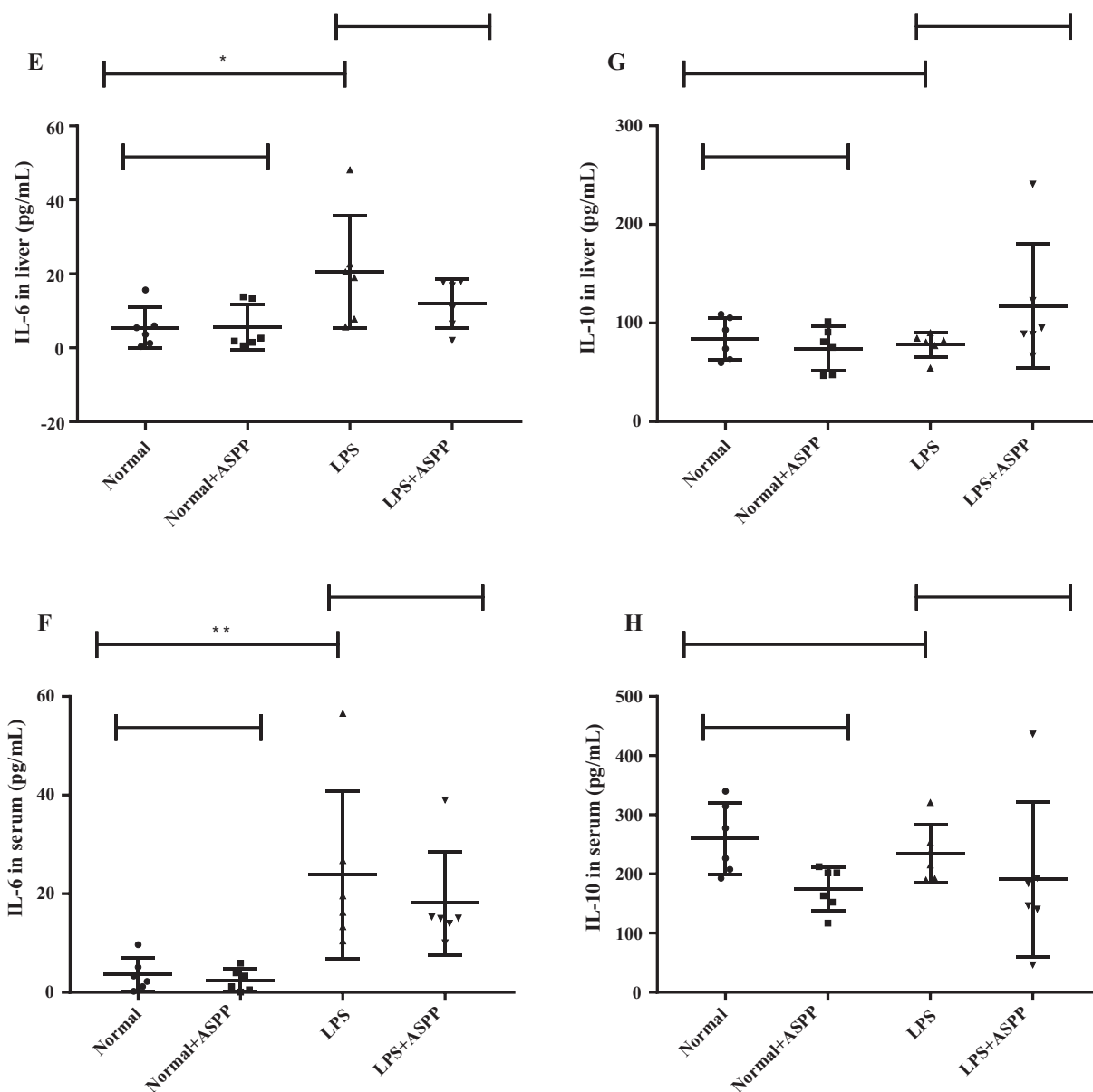


Fig. 6 (continued).

Jiangsu Province (No. BK20151310), Qing Lan Project of Jiangsu Province, China Agriculture Research System (CARS-10-B20) and Jiangsu Self-innovation Fund for Agricultural Science and Technology (No. CX [17] 2030).

References

- [1] A.R. Phull, S.J. Kim, Fucoidan as bio-functional molecule: insights into the anti-inflammatory potential and associated molecular mechanisms, *J. Funct. Foods* 38 (2017) 415–426.
- [2] S. Nepali, H.-H. Kim, J.-H. Lee, H.-Y. Lee, D.-K. Kim, Y.-M. Lee, Wheatgrass-derived polysaccharide has anti-inflammatory, anti-oxidative and anti-apoptotic effects on LPS-induced hepatic injury in mice, *Phytother. Res.* 31 (2017) 1107–1116.
- [3] M. Gasparri, T.Y. Forbes-Hernandez, F. Giampieri, S. Afrin, J.M. Alvarez-Suarez, L. Mazzoni, B. Mezzetti, J.L. Quiles, M. Battino, Anti-inflammatory effect of strawberry extract against LPS-induced stress in RAW 264.7 macrophages, *Food Chem. Toxicol.* 102 (2017) 1–10.
- [4] A.G.W. Gong, L.M.L. Zhang, C.T.W. Lam, M.L. Xu, H.Y. Wang, H.Q. Lin, T.T.X. Dong, K.W.K. Tsim, Polysaccharide of Danggui Buxue Tang, an ancient Chinese derbal decoction, induces expression of pro-inflammatory cytokines possibly via activation of NF- κ B signaling in cultured RAW 264.7 cells, *Phytother. Res.* 31 (2017) 274–283.
- [5] Y. Neelakandan, A. Venkatesan, Antinociceptive and anti-inflammatory effect of sulfated polysaccharide fractions from *Sargassum wightii* and *Halophila ovalis* in male Wistar rats, *Indian J. Pharmacol.* 48 (2016) 562–570.
- [6] Q. Liu, S. Xu, L. Li, T. Pan, C. Shi, H. Liu, M. Cao, W. Su, G. Liu, *In vitro* and *in vivo* immunomodulatory activity of sulfated polysaccharide from *Porphyra haitanensis*, *Carbohydr. Polym.* 165 (2017) 189–196.
- [7] D.-J. Chung, M.-Y. Yang, Y.-R. Li, W.-J. Chen, C.-Y. Hung, C.-J. Wang, Ganoderma lucidum repress injury of ethanol-induced steatohepatitis via anti-inflammation, anti-oxidation and reducing hepatic lipid in C57BL/6J mice, *J. Funct. Foods* 33 (2017) 314–322.
- [8] J. Jiang, F. Kong, N. Li, D. Zhang, C. Yan, H. Lv, Purification, structural characterization and *in vitro* antioxidant activity of a novel polysaccharide from Boshuzhi, *Carbohydr. Polym.* 147 (2016) 365–371.
- [9] A. Barad, S. Mackedenski, W.M. Li, X.J. Li, B.C.C. Lim, F. Rashid, L.E. Tackaberry, H.B. Massicotte, K.N. Egger, K. Reimer, P.C.K. Cheung, C.H. Lee, Anti-proliferative activity of a purified polysaccharide isolated from the basidiomycete fungus *Paxillus involutus*, *Carbohydr. Polym.* 181 (2018) 923–930.
- [10] Z. Mzoughi, A. Abdelhamid, C. Rihouey, D. Le Cerf, A. Bouraoui, H. Majdoub, Optimized extraction of pectin-like polysaccharide from *Suaeda frutescens* leaves: characterization, antioxidant, anti-inflammatory and analgesic activities, *Carbohydr. Polym.* 185 (2018) 127–137.
- [11] Q. Li, Y. Feng, W. He, L. Wang, R. Wang, L. Dong, C. Wang, Post-screening characterization and *in vivo* evaluation of an anti-inflammatory polysaccharide fraction from *Eucommia ulmoides*, *Carbohydr. Polym.* 169 (2017) 304–314.

- [12] J. Qi, S.M. Kim, Characterization and immunomodulatory activities of polysaccharides extracted from green alga *Chlorella ellipsoidea*, *Int. J. Biol. Macromol.* 95 (2017) 106–114.
- [13] K.B. Jeddou, F. Chaari, S. Maktouf, O. Nouri-Ellouz, C.B. Helbert, R.E. Ghorbel, Structural, functional, and antioxidant properties of water-soluble polysaccharides from potatoes peels, *Food Chem.* 205 (2016) 97–105.
- [14] Q. Wu, H. Qu, J. Jia, C. Kuang, Y. Wen, H. Yan, Z. Gui, Characterization, antioxidant and antitumor activities of polysaccharides from purple sweet potato, *Carbohydr. Polym.* 132 (2015) 31–40.
- [15] B. Yuan, X. Yang, M. Kou, C. Lu, Y. Wang, J. Peng, P. Chen, J. Jiang, Selenylation of polysaccharide from the sweet potato and evaluation of antioxidant, antitumor, and antidiabetic activities, *J. Agric. Food Chem.* 65 (2017) 605–617.
- [16] H. Yong, X. Wang, R. Bai, Z. Miao, X. Zhang, J. Liu, Development of antioxidant and intelligent pH-sensing packaging films by incorporating purple-fleshed sweet potato extract into chitosan matrix, *Food Hydrocoll.* 90 (2019) 216–224.
- [17] C. Tang, J. Sun, J. Liu, C. Jin, X. Wu, X. Zhang, H. Chen, Y. Gou, J. Kan, C. Qian, N. Zhang, Immune-enhancing effects of polysaccharides from purple sweet potato, *Int. J. Biol. Macromol.* 123 (2019) 923–930.
- [18] J. Sun, B. Zhou, C. Tang, Y. Gou, H. Chen, Y. Wang, C. Jin, J. Liu, F. Niu, J. Kan, C. Qian, N. Zhang, Characterization, antioxidant activity and hepatoprotective effect of purple sweet potato polysaccharides, *Int. J. Biol. Macromol.* 115 (2018) 69–76.
- [19] C. Tang, J. Sun, B. Zhou, C. Jin, J. Liu, J. Kan, C. Qian, N. Zhang, Effects of polysaccharides from purple sweet potatoes on immune response and gut microbiota composition in normal and cyclophosphamide treated mice, *Food Funct.* 9 (2018) 937–950.
- [20] J. Liu, X. Wen, J. Kan, C. Jin, Structural characterization of two water-soluble polysaccharides from black soybean (*Glycine max* (L.) Merr.), *J. Agric. Food Chem.* 63 (2015) 225–234.
- [21] T. Bitter, H.M. Muir, A modified uronic acid carbazole reaction, *Anal. Biochem.* 4 (1962) 330–334.
- [22] H. Zhu, L. Tian, L. Zhang, J. Bi, Q. Song, H. Yang, J. Qiao, Preparation, characterization and antioxidant activity of polysaccharide from spent *Lentinus edodes* substrate, *Int. J. Biol. Macromol.* 112 (2018) 976–984.
- [23] Z. Wen, X. Xiang, H. Jin, X. Guo, L. Liu, Y. Huang, X. OuYang, Y. Qu, Composition and anti-inflammatory effect of polysaccharides from *Sargassum horneri* in RAW264.7 macrophages, *Int. J. Biol. Macromol.* 88 (2016) 403–413.
- [24] Z. Wang, J. Xie, Y. Yang, F. Zhang, S. Wang, T. Wu, M. Shen, M. Xie, Sulfated *Cyclocarya paliurus* polysaccharides markedly attenuates inflammation and oxidative damage in lipopolysaccharide-treated macrophage cells and mice, *Sci. Rep.* 7 (2017), 40402.
- [25] G. Ma, W. Yang, A.M. Mariga, Y. Fang, N. Ma, F. Pei, Q. Hu, Purification, characterization and antitumor activity of polysaccharides from *Pleurotus eryngii* residue, *Sci. Rep.* 114 (2014) 297–305.
- [26] J. Liu, X. Wen, X. Zhang, H. Pu, J. Kan, C. Jin, Extraction, characterization and *in vitro* antioxidant activity of polysaccharides from black soybean, *Int. J. Biol. Macromol.* 72 (2015) 1182–1190.
- [27] H. Yong, X. Wang, J. Sun, Y. Fang, J. Liu, C. Jin, Comparison of the structural characterization and physicochemical properties of starches from seven purple sweet potato varieties cultivated in China, *Int. J. Biol. Macromol.* 120 (2018) 1632–1638.
- [28] Y. Chai, M. Zhao, Purification, characterization and anti-proliferation activities of polysaccharides extracted from *Viscum coloratum* (Kom.) Nakai, *Carbohydr. Polym.* 149 (2016) 121–130.
- [29] X. Shi, O. Li, J. Yin, S. Nie, Structure identification of α -glucans from *Dictyophora echinvolvata* by methylation and 1D/2D NMR spectroscopy, *Food Chem.* 271 (2019) 338–344.
- [30] C. Nie, P. Zhu, S. Ma, M. Wang, Y. Hu, Purification, characterization and immunomodulatory activity of polysaccharides from stem lettuce, *Carbohydr. Polym.* 188 (2018) 236–242.
- [31] A.F.D. Oliveira, G.E.D. Nascimento, M. Iacomini, L.M.C. Cordeiro, T.R. Cipriani, Chemical structure and anti-inflammatory effect of polysaccharides obtained from infusion of *Sedum dendroideum* leaves, *Int. J. Biol. Macromol.* 105 (2017) 940–946.
- [32] K.K.A. Sanjeewa, I.P.S. Fernando, S.-Y. Kim, H.-S. Kim, G. Ahn, Y. Jee, Y.-J. Jeon, *In vitro* and *in vivo* anti-inflammatory activities of high molecular weight sulfated polysaccharide; containing fucose separated from *Sargassum horneri*: short communication, *Int. J. Biol. Macromol.* 107 (2018) 803–807.
- [33] Y. Zhang, Y. Zeng, Y. Men, J. Zhang, H. Liu, Y. Sun, Structural characterization and immunomodulatory activity of exopolysaccharides from submerged culture of *Auricularia auricula-judae*, *Int. J. Biol. Macromol.* 115 (2018) 978–984.
- [34] I.d.L. Bezerra, A.R.C. Caillot, L.C.G.F. Palhares, A.P. Santana-Filho, S.F. Chavante, G.L. Sasaki, Structural characterization of polysaccharides from *Cabernet Franc*, *Cabernet Sauvignon* and *Sauvignon Blanc* wines: anti-inflammatory activity in LPS stimulated RAW 264.7 cells, *Carbohydr. Polym.* 186 (2018) 91–99.
- [35] H.M. Rajagopal, S.B. Manjegowda, C. Serkad, S.M. Dharmesh, A modified pectic polysaccharide from turmeric (*Curcuma longa*) with antiulcer effects via anti-secretory, mucoprotective and IL-10 mediated anti-inflammatory mechanisms, *Int. J. Biol. Macromol.* 118 (2018) 864–880.
- [36] D.Y.-W. Fann, Y.-A. Lim, Y.-L. Cheng, K.-Z. Lok, P. Chunduri, S.-H. Baik, G.R. Drummond, S.T. Dheen, C.G. Sobey, D.-G. Jo, C.L.-H. Chen, T.V. Arumugam, Evidence that NF- κ B and MAPK signaling promotes NLRP inflammasome activation in neurons following ischemic stroke, *Mol. Neurobiol.* 55 (2018) 1082–1096.
- [37] J. Park, C.-H. Kwak, S.-H. Ha, K.-M. Kwon, F. Abekura, S.-H. Cho, Y.-C. Chang, Y.-C. Lee, K.-T. Ha, T.-W. Chung, C.-H. Kim, Ganglioside GM3 suppresses lipopolysaccharide-induced inflammatory responses in RAW 264.7 macrophage cells through NF- κ B, AP-1, and MAPKs signaling, *J. Cell. Biochem.* 119 (2018) 1173–1182.